A METHODOLOGY TO ASSESS ROBUST STABILITY AND ROBUST PERFORMANCE OF AUTOMATIC FLIGHT CONTROL SYSTEMS

Alex Sander Ferreira da Silva[*]
sander.silva@embraer.com.br

Henrique Mohallem Paiva[†]
hmpaiva@mectron.com.br

Karl Heinz Kienitz[‡]
kienitz@ieee.org

[*] Empresa Brasileira de Aeronáutica (EMBRAER) - Sistemas de Comando de Voo
Av. Brigadeiro Faria Lima, 2170 – São José dos Campos, SP – 12227-901 – Brasil
Tel: +55 12 3927-0277, Fax: +55 12 3927-4525

[†] Mectron Engenharia, Indústria e Comércio S/A. - Gerência de Engenharia de Sistemas
Av. Brigadeiro Faria Lima, 1399 – São José dos Campos, SP – 12227-000 – Brasil
Tel: +55 12 2139-3500, Fax: +55 12 2139-3535

[‡] Instituto Tecnológico de Aeronáutica (ITA) - Divisão de Engenharia Eletrônica
Praça Marechal Eduardo Gomes, 50 – São José dos Campos, SP – 12228-900 – Brasil
Tel: +55 12 3947-6931, Fax: +55 12 3947-6930

RESUMO

Uma metodologia para avaliar a estabilidade e o desempenho robustos de sistemas automáticos de comando de voo

Esse artigo apresenta uma metodologia para avaliar a estabilidade robusta e o desempenho robusto de sistemas automáticos de comando de vôo. A ferramenta matemática utilizada na metodologia proposta é o valor singular estruturado, μ. Para fins de comparação, o artigo utiliza uma metodologia largamente utilizada na indústria aeronáutica para mensurar as características mencionadas. Os problemas dessa metodologia são discutidos e é mostrado que o método proposto é uma elegante alternativa para contornar as desvantagens do método industrial. Um procedimento passo a passo é apresentado, incorporando as vantagens da abordagem atualmente utilizada na indústria e eliminando suas fraquezas.

PALAVRAS-CHAVE: Controle Robusto, Valor Singular Estruturado, Realimentação, Sistemas Automáticos de Comando de Voo

ABSTRACT

This article presents a methodology to assess the robust stability and the robust performance of automatic flight control systems (AFCS). The mathematical tool used in the proposed methodology is the structured singular value, μ. For comparison purposes, the paper uses a method largely employed in the aircraft industry to measure the quoted AFCS attributes. The issues existing in this methodology are discussed and it is shown that the proposed method presents one elegant path to deal with the mentioned drawbacks. A step by step procedure is provided, incorporating the advantages offered by the approach currently used in the industry and eliminating its weaknesses.

KEYWORDS: Robust Control, Structured Singular Value, Feedback Systems, Automatic Flight Control Systems

Artigo submetido em 09/11/2010 (Id.: 01217)
Revisado em 29/01/2011, 24/03/2011
Aceito sob recomendação do Editor Associado Prof. Luis Fernando Alves Pereira

1 INTRODUCTION

Modern automatic flight control systems (AFCS) design and analysis is a model-based activity. This means that, in a preliminary step, it is necessary to develop aircraft models as well as the models of the aircraft main peripherals, like actuators, engines, etc. Modeling comprises a vast engineering area and its detailed discussion lies beyond the scope of this paper. Fortunately there is an extensive and rich literature presenting the main aspects of aircraft modeling (Cook, 2007; Pamadi, 2004; Phillips, 2004; Roskam, 2003; Roskam and Lan, 2003; Stevens and Lewis, 2003; Yechout and Morris, 2003).

One important output of the modeling activity is the understanding of the possible inaccuracies that might be present in the particular model under study. This knowledge can be applied during the design phase in order to minimize the possibility of AFCS rework during the final flight test phase, since it is well known that major changes during this stage are time consuming and expensive.

Broadly speaking, the robustness assessment consists in verifying if the required performance and stability are maintained, considering all possible plant variations within their assumed bounds. Such verification does not depend on the particular choice of the AFCS design synthesis technique. In fact, they can even be used as judgment criteria of the quality of a specific AFCS controller.

Since having reliable measures of control law robustness is an unquestionable necessity, flight control laws designers keep a constant interest on the subject. A procedure to check AFCS robustness largely used in the aeronautical industry employs the concept of open loop transfer functions (Gangsaas, Blight and Caldeira, 2008; Gangsaas et al., 2008). This article revisits this procedure and points out its limitations. The subsequent focus is to show how the concept of structured singular value μ can be used to fill in the existing gaps. The final goal is to provide a step by step methodology which incorporates the advantages offered by the currently used method and eliminates its weaknesses.

The text is organized as follows. Section 2 presents a general layout, applicable to a broad class of AFCS control laws. It also identifies the AFCS elements responsible for guaranteeing robustness. Section 3 provides a short description of one particular AFCS. It also presents the aircraft models, valid for one flight condition, as well as the adopted modeling of the flight controls elements. Section 4 discusses a method widely used in the aircraft industry to assess AFCS robust stability and performance. Section 5 provides the add-ons sufficient to overcome the present limitations of the method from Section 4. The analysis plots provided in Section 4 and 5 are based on the models described in Section 3. Final remarks are given in Section 6.

2 AFCS GENERAL LAYOUT

The model arrangement depicted in Fig.1 shows the architecture of a real AFCS application (aircraft, sensors, actuators, flight control computer, pilot, etc). Aircraft dynamics is represented by a multiple-input multiple-output (MIMO) system, having as inputs U_1, U_2, ..., U_p and as outputs the signals In_1, In_2, In_3, ..., In_n. The sensors dynamics are located inside the block *Sensor Models*.

The AFCS control law uses the measured signals S_1, S_2, ..., S_n and the reference signals R_1, R_2, ..., R_t, which are provided either by the pilot or by the navigation computer. The control algorithm provides the demands for the aircraft inputs, $ComU_1$, $ComU_2$, ..., $ComU_p$. Pure time delays, representing either the data transportation on digital buses or the computer calculation lag, are also implemented inside the block *AFCS*.

Figure 2 shows a general AFCS layout. The signal preprocessing block computes the signals estimate to be used in the control law. It takes the available measurement from the aircraft sensors and performs data computation and filtering. The set-point generator computes the feedback setpoints, based on either the pilot or navigation computer inputs. Finally, the feedback section computes the aircraft inputs demands based on the errors between the estimated variables and the respective set-points.

The sensed signals used by the control algorithm, S_{1d}, S_{2d}, ..., S_{nd}, are the delayed version of the sensor outputs. This delay is due to the transport delay inherent to digital buses. The aircraft input demands produced by the control law, $ComU_{1u}$,$ComU_{2u}$,..., $ComU_{pu}$, also suffer a delay prior to reaching the actuators.

The control strategy encapsulated in Fig. 2 is a two degree of freedom control law structure (Araki and Taguchi, 2003). Two major responsibilities shall be addressed by the subsystem containing the feedback component and the data preprocessing, namely the disturbance rejection and the assurance of overall system robustness. It means that these are the elements which are tested during the robustness checks.

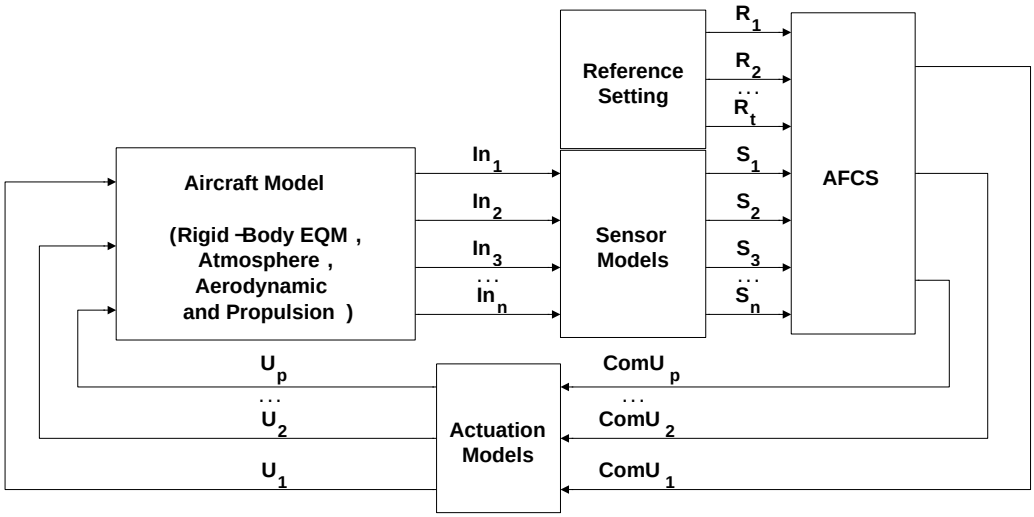

Figure 1: Model Arrangement - Overview

3 SHORT DESCRIPTION OF ONE SPECIFIC AFCS

The AFCS which is presented in this section is an example of a ψ hold/ψ capture control law. In other words, this is an auto pilot function which holds the desired heading and also allows the proper transitions from one initial heading to the final one.

Another function of this AFCS is the regulation of the side slip angle, β, around zero. This feature is important for two basic reasons: 1 - This is what damps out the aircraft Dutch roll mode. 2 - Compared to a simple regulator of $\dot{\beta}$ (which comprises the conventional *Yaw damper* of commercial aircraft), a regulator of β provides the same features and also the automatic trimming of the aircraft lateral axis.

The objective is not to present how this final design was achieved. The goal is to provide a design, with performance compatible with a good auto pilot, and then use it to aid in the presentation of the methods described in Sections 4 and 5.

3.1 Aircraft Dynamics

A non-linear model of the Boeing 747 aircraft was assembled using Matlab/Simulink. For a detailed description of this aircraft model, the reader is referred to the chapter 2 of the master thesis (Silva, 2009).

A standard Von Karman wind turbulence model is also implemented. In this model, turbulence is generated by passing band-limited white noise through appropriate filters, as specified in detail in (DoD, 1990).

Together with the non-linear model, a series of Matlab scripts was prepared to automate the routines necessary for the design and analysis of flight control laws. Two of these functions perform the trimming and the linearization around the trimming condition.

The analysis on Sections 4 and 5 are based on two linear latero-directional models, which represents the two extreme mass configurations available in one flight condition. Table 1 presents the flight condition and the description of the mass configurations.

Table 1: Linear Models - Flight Condition and Mass Configurations

Parameter	Model 1	Model 2
Mass [kg]	181440	317510
$\mathbf{CG}_{POS}$ (1) [%]	25	25
$\mathbf{V}_{CAS}$ [kn]	244	244
$\mathbf{h}_p$ [ft]	20000	20000

(1) Center of gravity position, in the longitudinal axis

The inputs of the linear aircraft models are aileron and rudder position, and the outputs are side slip angle (β), bank angle (ϕ), roll rate (p), yaw rate (r), lateral acceleration at the center of gravity location (A_YCG) and heading (ψ).

3.2 Sensor Models

The output of each sensor carries not only the aircraft specific parameter dynamics, but also has some spurious dynamics due to the sensing device itself. The lesser the contamination of the data with the sensor dynamics and with sensor noise, the better the specific sensor signal.

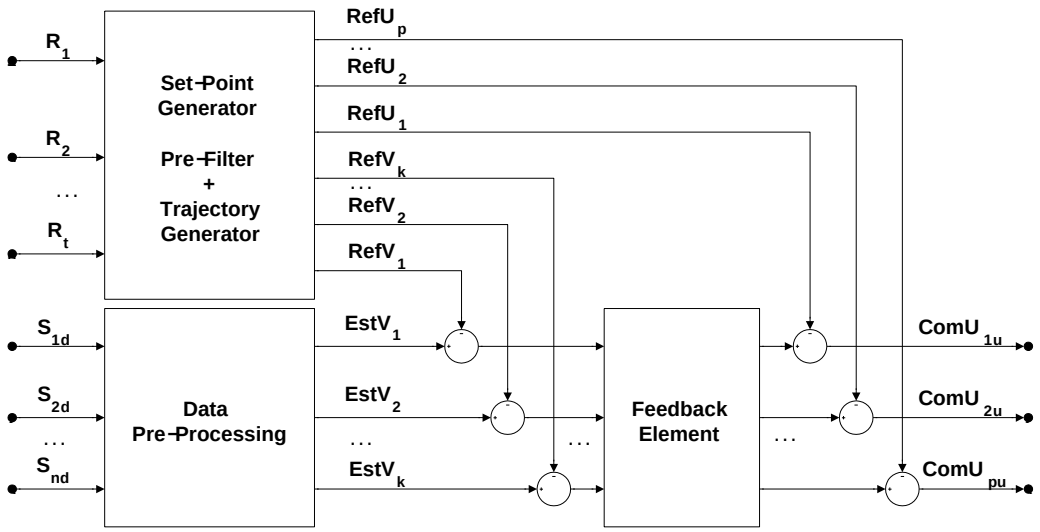

Figure 2: AFCS General Structure

In this study, the sensors are modeled as a second order lag plus one pure time delay. For linear analysis purposes, the pure time delays are replaced by second order Pade approximation (Stevens and Lewis, 2003). Table 2 presents the adopted values of the second order lag natural frequency (ω_n), the associated poles damping ratio (ζ) and the pure time delay value.

Table 2: Sensor dynamics values

Sensed Signal	ω_n [rad/s]	ζ	Delay [ms]
ψ	94.2	1.0	20
ϕ	94.2	1.0	20
p	75.4	1.0	10
r	75.4	1.0	10
A_{YCG}	50.3	1.0	10
β	12.0	0.7	20

3.3 Actuation Models

A practical AFCS design must also take into account the limitations imposed by the actuation system. This system can be mathematically described by an input-output relationship between the intended and actual positions.

In this study, the actuators are modeled as a second order lag. Table 3 presents the adopted values of the second order lag natural frequency (ω_n), the associated poles damping ratio (ζ) and the actuator steady state-gain (K).

3.4 AFCS Computer

At the present time, the flight control laws are almost invariably implemented in digital computers. The primary advantage in following this approach is the flexibility in executing complex data manipulations.

Table 3: Actuation system Values

Input	K	ω_n [rad/s]	ζ
Aileron	1	31.4	0.7
Rudder	1	31.4	0.7

One shortcoming is the pure time delay which is added due to the nature of digital calculations. Nevertheless, this drawback is of secondary order today and it tends to become meaningless in the future, as the computer capacity is rapidly increasing.

Table 4 presents the adopted transport delays from sensor to the AFCS computer. In real applications, these values are dictated by the priority assigned for each signal, given the limitation imposed by the capacity of the particular digital bus used.

Table 4: Transport delay from Sensor to AFCS computer

Signal	ψ	ϕ	p	r	A_{YCG}	β
Delay [ms]	20	20	10	10	10	20

The computation lag is represented by a 25 ms delay, added at the output of the control law algorithm. Since the control laws are digitally implemented, the effects of the sampler plus the zero order hold (ZOH) must also be accounted for.

For linear analysis purposes, the pure time delay is replaced by a second order Pade approximation, while the ZOH is replaced by a first order approximation. These approximations can be found in (Stevens and Lewis, 2003).

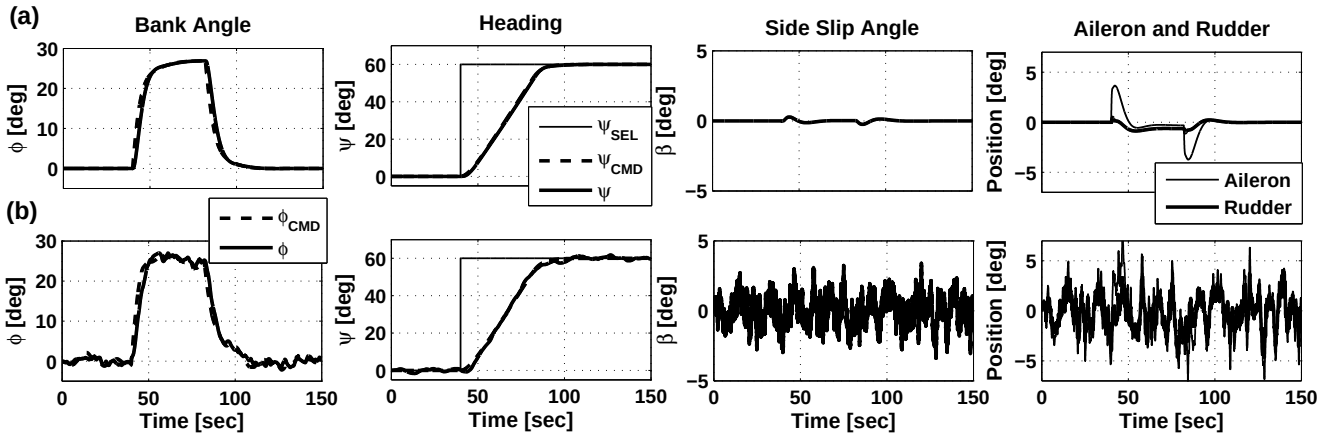

Figure 3: Time History - ψ transition and ψ hold: (a) without turbulence, (b) with severe turbulence.

3.5 AFCS Function

The objective of this subsection is to provide some additional information on how this specific AFCS (ψ hold/ψ capture) works. It also provides evidences that this studied design has a performance compatible with a good autopilot.

This AFCS uses aileron and rudder to control ψ and β. Figure 3 (a) shows the time history for a ψ transition, from 0 deg to 60 deg. The pilot input is represented by the ψ_{SEL} curve, which is the output of a ψ knob, located in the cockpit. The ψ_{CMD} is the set-point on ψ, which is generated based on the ψ_{SEL} signal. The ϕ_{Cmd} is the set-point on bank-angle. This signal is the command sent by the autopilot *outer loop* to the autopilot *inner loop*.

The plots in Fig. 3 (a) were generated considering model 1 (see Table 1) and atmospheric conditions without any turbulence. Figure 3 (b) refers to the same model, but now including a severe turbulence level. Similar results are achieved when using model 2 of Table 1.

The basic conclusion from these plots is that this control law is able of performing the ψ transition as well as the ψ hold in a desired fashion, even when the strongest possible turbulence level is included.

4 CURRENT INDUSTRIAL METHOD TO ASSESS ROBUSTNESS

In order to help out in the subsequent explanations, the following definitions, valid in the context of this work, are introduced:

Open Loop Transfer Function($OLTF$): It is the single-input single-output (SISO) system obtained after the closed loop system is opened at one control law designated location. The particular point where this procedure is carried out can be one of the following: 1 - any sensor input used by the control law; 2 - any of the aircraft inputs used by the control law; 3 - any internal point of the control law block diagram. The abbreviation $OLTF_{In_2}$ denotes open loop transfer function at the signal In_2, as illustrated in Fig. 4.

Regulated Variable(RV): It is one aircraft variable whose steady state value shall be controlled by the AFCS. One example is the pressure altitude, in an altitude hold control law.

4.1 Robust Stability

A solution is considered to possess robust stability (RS) if the OLTF of every one of the sensor inputs $OLTF_{In_1}$, ..., $OLTF_{In_n}$ and of the aircraft inputs inputs ($OLTF_{U_1}$, ..., $OLTF_{U_p}$) have certain characteristics.

The quoted characteristics are extracted from the magnitude versus phase plot, applied to the transfer function -OLTF. The test consists in a graphical check of these transfer functions against a pre-defined template, which can be modified in accordance with the problem in hand.

Figure 5 (a) presents one example of a case which passes the robustness criterion, while Fig. 5 (b) presents a failed one. The dashed curve is constructed around the critical point, marking the so called *robustness boundary*. In this case, straight lines connects the $\pm$ 6 db gain margin with the $\pm$ 45 degrees phase margin points. These values, as well as the shape of this boundary, can be modified, without effect on the following discussion.

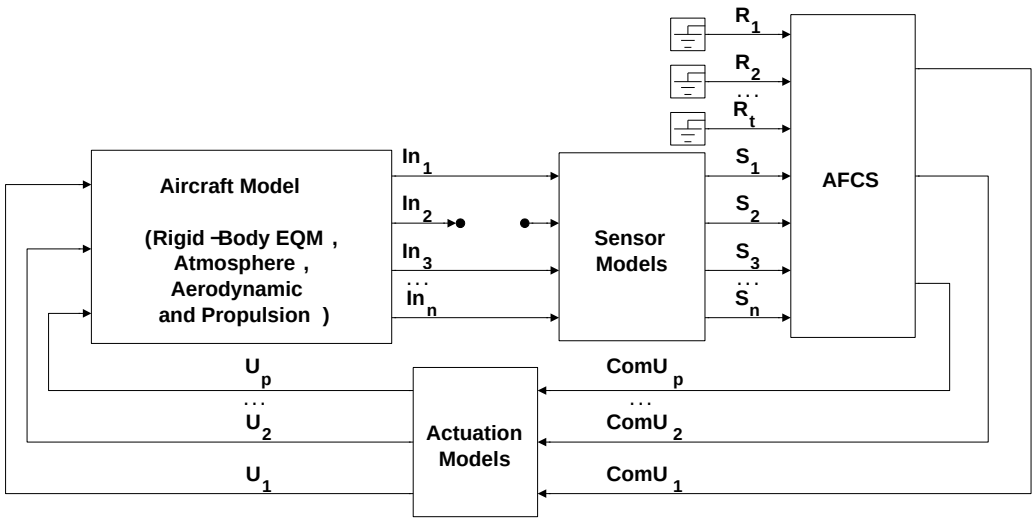

Figure 4: Illustration of the building up of one OLTF

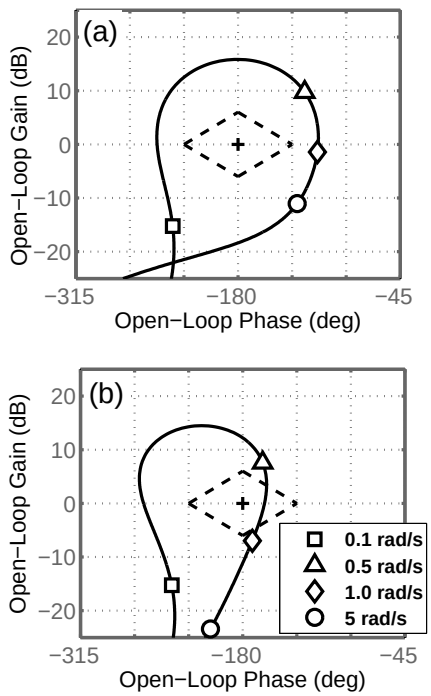

Figure 5: Magnitude Versus Phase Plot - (a) Success and (b) Fail in the Robustness test

As already mentioned, this robustness check is a widespread procedure employed in the aircraft industry. Examples employing a similar robustness check methodology can be found in (Gangsaas, Blight and Caldeira, 2008; Gangsaas et al., 2008; Garteur, 1996). Nevertheless, there are issues on this method, which are discussed in the sequence.

The basic concept behind this process is the Nyquist Stability Criterion (Ogata, 2002), applied to SISO systems. The robustness boundary is set as the region, around the critical point, that shall be avoided. The further is the $-OLTF$ plot to the critical point, the more robust is the closed loop system.

This concept, which is the same as the gain and phase margin check, is a powerful tool, which can be readily applied to any SISO system. Applying this to the described $OLTFs$, extracted out from a MIMO system, is an extrapolation which can present issues (Skogestad and Postlethwaite, 2007). Problems may arise since this concept assumes that each loop is modified without any perturbation on the other loops. One particular example where this assumption is valid is the case where there is either an unknown scale factor or an unknown additional time delay applied to only only one of the sensors signals. However, this assumption is not valid in the general case, because a model inaccuracy tends to affect all the loops simultaneously.

One approach to minimize the concerns described above consists in checking the $OLTF$ at the extremes of the mass and center of gravity (CG) envelope, for a given flight condition. The idea is to make sure that the same level of margins is kept, regardless of the mass configuration under study. This practice adds mores confidence on the robustness test, since not only one nominal model is checked. Instead, a set of models, representative of the mass and CG envelope, is tested simultaneously.

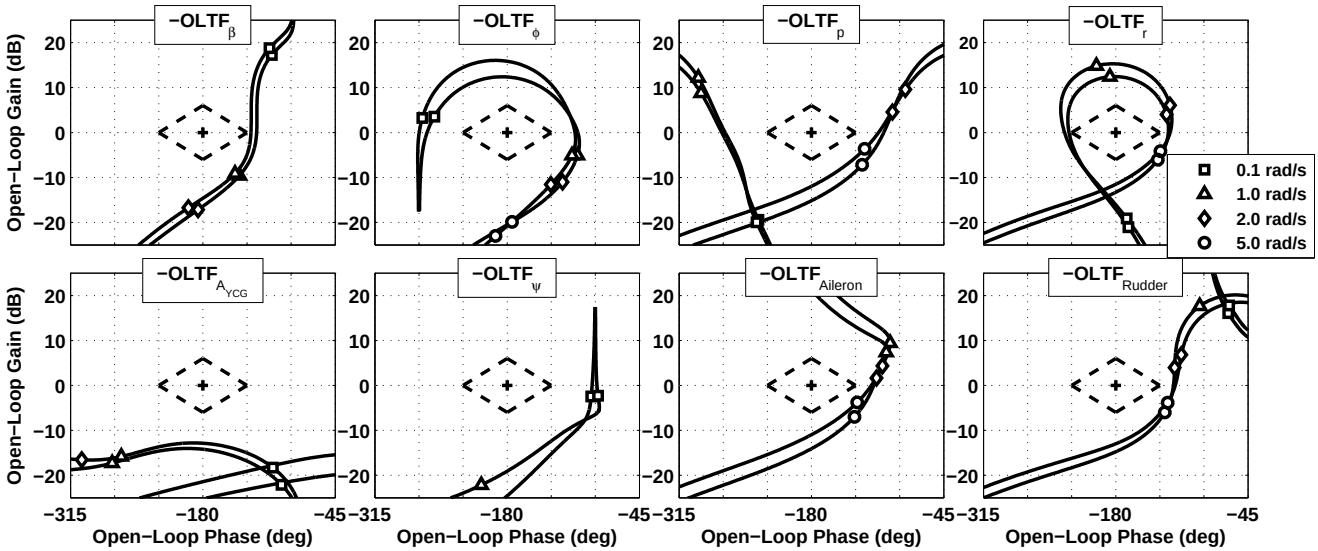

Figure 6: Magnitude Versus Phase Plot - ψ hold/ψ capture control law

As an illustration of this approach, Figure 6 provides the magnitude versus phase plots of the ψ hold/ψ capture control law. The two curves on each plot represent the two mass configurations of Table 1.

Nonetheless, no mathematical proof can be given by this approach. One elegant procedure to overcome this weakness can be achieved by using the structured singular value, called here μ_Δ. This approach will be further discussed in Section 5.

4.2 Robust Performance

A solution is considered to possess nominal performance (NP) if the error between the regulated variables and their respective set-points are kept inside a pre-defined limit, even under the maximum expected disturbances.

The adopted nominal performance test consists in first assembling the frequency responses of the SISO systems, corresponding to all aircraft inputs and regulated variables, following the idea illustrated in Fig. 7 for input U_1. The subsequent step is to compare the magnitude plots of these SISO systems against defined upper boundaries. The overall system is regarded to have nominal performance if the described plots are all below their respective upper limits.

A robust performance test consists in performing the same checking on the extremes of the mass and CG envelope for each given flight condition. It can also be decided to add a grid of aircraft models with either delay or scale factor perturbations applied to its inputs and outputs. Each point of this gridding shall be inside the space of all possible delay and scale factor variations.

Two issues arise in using this robust performance test. The first one is that the number of models to be tested increases to a prohibitive amount as the number of uncertain parameters increases. The second issue is that no mathematical certainty can be given when following this approach, even when the number of point in the grid is made extremely refined. This is so because a worse case can be located in between two points of the chosen grid.

The concept of μ_Δ, which is discussed in Section 5, can be applied to better assess the robust performance of the AFCS.

5 COMPLETING THE ROBUSTNESS TEST

There is an extensive amount of publications about linear fractional transformations (LFT) and μ (Chenglong, Xin and Chuntao, 2010; Hsu et al, 2008; Menon, Bates and Postlethwaite, 2007; Menon et al, 2009; Pfifer and Hecker, 2011; Natesan and Bhat, 2007; Yun and Han, 2009; Zhou et al, 2007). The objective of this section is to make use of the well-established characteristics of these tools, with the final target of proposing one set of tests to measure the robust stability and performance.

Firstly, a short review of LFT and μ is provided. The related terminologies, which are applied in this work, are introduced in this stage. The subsequent step is the definition of the

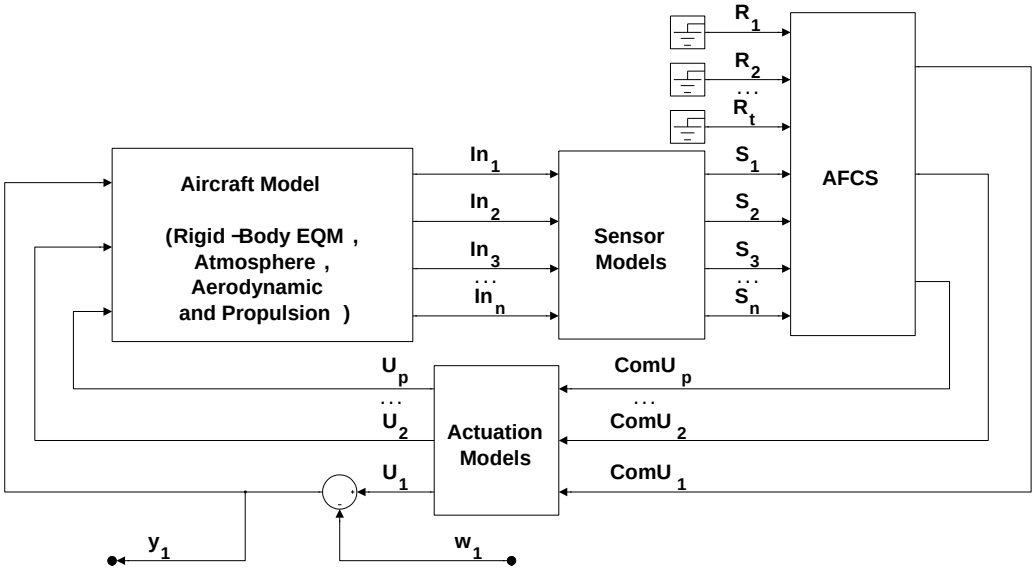

Figure 7: One of the SISOs systems used for measuring the nominal performance of the feedback system.

quoted robustness tests. For illustration purposes, the defined tests are then applied to the ψ hold/ψ capture control law.

5.1 Short review of LFT and μ

The starting point for the robustness analysis is a system representation in which the uncertain perturbations are lumped into a block diagonal matrix, as represented in Eq. (1).

$$\Delta = diag\{\Delta_i\} \tag{1}$$

When following this approach, for the particular case of control law analysis, it is sufficient to use the $N\Delta-$Structure (Skogestad and Postlethwaite, 2007) depicted in Fig. 8.

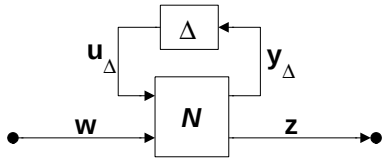

Figure 8: $N\Delta-$Structure for robust performance analysis

In Fig. 8, N is the generalized plant, including the controller, w is a vector representing the exogenous inputs (which can be weighted) and z is a vector representing the exogenous output (which may also be weighted). The Δ matrix, representing the system perturbations, is built in a way to satisfy $\|\Delta\|_\infty \leq 1$.

The transfer function matrix from w to z, $z = Fw$, is related to N and Δ by an upper LFT, as shown in Eq. (2).

$$\begin{array}{rcl} F & = & F_u(N,\Delta) \triangleq \\ & \triangleq & N_{22} + N_{21}\Delta\left(I - N_{11}\Delta\right)^{-1} N_{12} \end{array} \tag{2}$$

where the N matrix is partitioned as in Eq. (3) to be compatible with Δ. N_{22} represents the nominal transfer function from w to z (Skogestad and Postlethwaite, 2007).

$$N = \left[\begin{array}{cc} N_{11} & N_{12} \\ N_{21} & N_{22} \end{array} \right] \tag{3}$$

The definition of the structured singular value of a complex matrix M, for the allowed structure Δ, is presented in Eq. (4).

$$\mu\left(M\right)^{-1} \triangleq \min\{\bar{\sigma}\left(\Delta\right) \mid \det\left(I - M\Delta\right) = 0 \quad \text{for structured } \Delta\} \tag{4}$$

Clearly $\mu(M)$ depends not only on M, but also on the allowed structure for Δ. For this reason, it is preferable to use the notation $\mu_\Delta(M)$. In words, $\mu_\Delta(M)$ is the reciprocal of the smallest structured Δ (with $\bar{\sigma}$ as the norm) that can be found and that can makes the matrix $(I - M\Delta)$ singular.

Finally, let the robust performance requirement be $\|F\|_\infty \leq 1$, for all allowable perturbations. Based on the terms defined

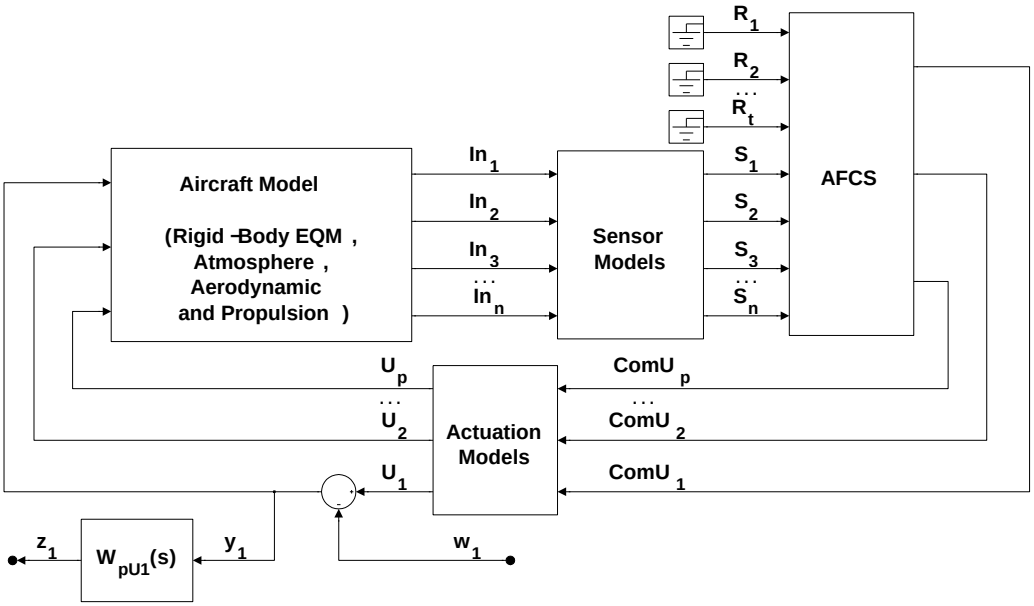

Figure 9: $N_{22}^{U_1}$ component of the N^{U_1} transfer matrix

on this section, it is possible to formulate the robust stability (RS) and the robust performance (RP) in terms of the conditions stated in Eq. (5) and (6) (Skogestad and Postlethwaite, 2007).

$$RS \Leftrightarrow \mu_{\Delta}\left(N_{11}\right) < 1,\ \forall\omega,\ \text{and NS satisfied} \qquad (5)$$

$$RP \Leftrightarrow \left| \begin{array}{l} \mu_{\tilde{\Delta}}\left(N\right) < 1,\ \forall\omega, \\ \tilde{\Delta} = \left[\begin{array}{cc} \Delta & 0 \\ 0 & \Delta_P \end{array} \right], \\ \text{and NS satisfied} \end{array} \right. \qquad (6)$$

where NS means nominal stability, which is verified by the simple check of all the closed loops poles real part. Δ_P is a full complex matrix, which has dimension compatible with the vectors w and z.

5.2 Proposed tests based on μ

The RS test is based on Eq. (5), while the RP test is based on Eq. (6). To use these equations, it is first necessary to put the control problem into the structure of Fig. 8.

The selected strategy consists in assembling one set of Ns. The component N_{11} is common to all elements of this set. The N_{22} partition is always a SISO model.

Figure 9 shows $N_{22}^{U_1}$, which corresponds to the weighted transfer function of an external disturbance on U_1 to the actual U_1. The weight W_{pU1} establishes how fast the disturbance is to be removed by the feedback component.

The transfer function $1/W_{pU1}$ represents an upper limit to the transfer function of w_1 to y_1, considering all the possible perturbations. The general shape of $1/W_{pU1}$ is a wash-out filter.

Following the same procedure, $N_{22}^{U_p}$ is established for all aircraft inputs. The weight selected for each aircraft input depends on the required attenuation, per frequency, of all the external disturbances on the given input. In other words, the weight characteristics for each aircraft input become an engineering requirement.

Additionally, $N_{22}^{RV_p}$ is also created, corresponding to the weighted transfer function of an external disturbance on RV_p to the actual RV_p. In this case, the weight choice is also based on the engineering requirement dictating how fast the external disturbance shall be removed from the given regulated variable.

For the example of the ψ hold/ψ capture control law, the regulated variables are ψ and β and the aircraft inputs are aileron and rudder. This means that, for this particular case, the RP test is based on the analysis of four LFTs: $\mu_{\tilde{\Delta}}(N^{\beta})$, $\mu_{\tilde{\Delta}}(N^{\psi})$, $\mu_{\tilde{\Delta}}(N^{Aileron})$ and $\mu_{\tilde{\Delta}}(N^{Rudder})$.

As already mentioned, the N_{11} component is the same for all the elements inside the set of Ns. This component is assembled as follows:

1. Add the perturbation weight described in Fig. 10 (a) for all aircraft outputs which have phase type inaccuracy. The value of τ_d represents the maximum expected additional delay, in seconds, that might be present on the particular signal;

2. Add the perturbation weight described in Fig. 10 (b) for all aircraft outputs which have scale factor type inaccuracy. The value of f_{Signal} represents the maximum expected scale factor that might be present on the particular signal;

3. Repeat items number 1 and 2, but now for all of the aircraft inputs.

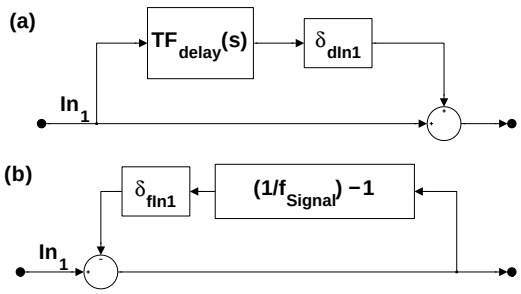

Figure 10: Perturbation due to (a) delay inaccuracy and (b) scale factor inaccuracy

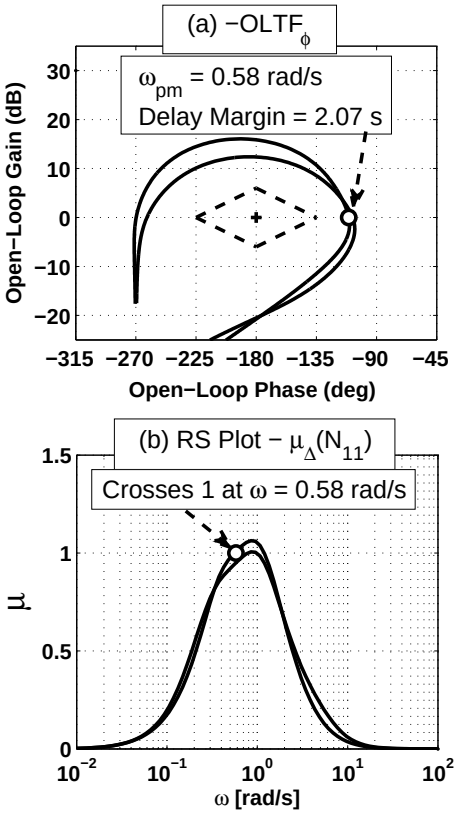

Figure 11: μ Validation

In Fig. 10, δ_{dIn1} represents an uncertain complex gain and δ_{fIn1} represents an uncertain real gain. The magnitudes of both δ_{dIn1} and δ_{fIn1} are limited to be less than or equal to 1. The transfer function $TF_{delay}(s)$ has the general format described in Eq. (7) (Skogestad and Postlethwaite, 2007).

$$TF_{delay}(s) = \left(\frac{2\tau_d s}{\tau_d s+2}\right)\left(\frac{\tau_d^2 s^2+2(0.838)2.363\tau_d s+(2.363)^2}{\tau_d^2 s^2+2(0.685)2.363\tau_d s+(2.363)^2}\right) \quad (7)$$

For the particular case where it is assumed the existence of inaccuracy in only one loop, it can be shown that the result of RS via μ leads to the same conclusion of the OLTF phase and gain margin check. As an example of this feature, Figure 11(a) shows the magnitude versus phase plot of the $-OLTF_\phi$, which shows a phase margin of 69.2 deg at 0.58 rad/s, corresponding to an equivalent delay margin of 2.07 s. Figure 11(b) shows the $\mu_\Delta(N_{11})$, considering that the only source uncertainty is the delay on the ϕ loop and that the maximum expected inaccuracy corresponds to T_{Signal} = 2.07 s. The plot of $\mu_\Delta(N_{11})$ crosses 1 at the phase margin frequency provided by the $-OLTF_\phi$ plot.

Similar results are achieved considering phase perturbations on the other loops, as well as gain factor perturbations. Therefore, when it is considered inaccuracy in only one loop at each time, the conclusion based on the μ analysis produces the same result as the margins checks of the $OLTF$. However, the μ analysis allows the additional check of simultaneous perturbations in a straightforward manner.

5.3 Results of ψ hold/ψ capture control law

In order to exercise the concepts presented in this section, the ψ hold/ψ capture controls law was tested, considering the maximum model inaccuracies as described on Table 5.

Table 5: Model inaccuracy factors

Signal	τ_d [s]	f_{Signal} [ADM]
ψ	0.020	1.00
ϕ	0.020	1.00
p	0.010	1.00
r	0.010	1.00
A_{YCG}	0.010	1.00
β	0.020	1.00
Aileron	0.010	1.15
Rudder	0.010	1.15

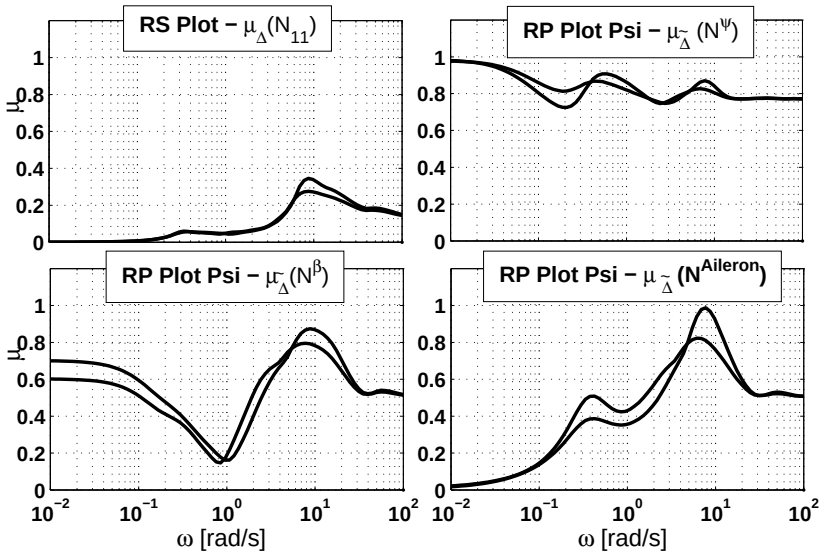

Figure 12: μ results

The selected performance weights have the general format described in Eq. (8). The parameters values for each specific weight are given in Table 6.

$$W_p(s) = \frac{1}{a_p}\left(\frac{\tau_p s + 1}{\tau_p s}\right) \tag{8}$$

Table 6: Performance weight parameters

Signal	ψ	β	Aileron
τ_p [s]	10	1.5	1.0
a_p [ADM]	1.3	2.0	2.0

In this design, the rudder demand is obtained exclusively from the β feedback components (proportional, integral and derivative components of β). For this reason, N^{β} is the same as N^{Rudder}. The final results are shown in Fig. 12. One important note is that each μ plot shown on this article is in fact an upper bound on the respective μ.

5.4 Discussion

The current industrial method has the drawback of assuming that the model inaccuracy is applied in only one of the loops. This can be the case sometimes, but, in the general situation, there may be errors in each of the aircraft inputs or sensor inputs. The actual error can be the result of any of the possible combinations.

The proposed additional tests, based on the concept of μ_{Δ}, allows the determination, in one go, of the worst combination of the possible errors, in terms of hampering the final stability and performance.

The proposed final procedure combines the two presented methodologies. The reason is that -OLTFs magnitude versus phase plot can be used not only as robustness measurement tool of individual loops inaccuracy, but also as a instrument for guiding the control law loop shaping, obtained via phase shift and/or gain increase/decrease of the -OLTFs. One important result of the proper OLTFs loop shaping is the fact that the damping of the closed loop poles are intimately linked with the proximity of these curves to the critical point.

The supplementary tests, based on μ_{Δ}, work as a complement for the current methodology, since it fulfills the existing gap. It does not provide the same aid in terms of indicating the best strategy for the control law loop shaping, but it provides the correct assurance of robust stability and performance for the most common situation, where the inaccuracies may happen simultaneously in multiple loops.

Another interesting usage of the μ_{Δ} robust performance test is that it allows the arbitration of the best control law among a set of control laws, which were generated following different design approaches.

6 CONCLUSIONS

This paper reviewed a method to check AFCS robustness largely used in the aeronautical industry, and pointed out its limitations. A complementary approach, based on the concept of structured singular value μ, was presented. The final procedure combines the advantage of both approaches. A

step by step procedure was presented, illustrating the use of the method.

ACKNOWLEDGEMENTS

The authors would like to thank the Brazilian agency CNPq (research fellowships) and the Brazilian companies Embraer and Mectron for their support.

REFERENCES

Araki, M. and Taguchi, H. (2003). Two-Degree-of-Freedom PID Controllers, *International Journal of Control, Automation, and Systems* **1**(4):401-411.

Chenglong, H., Xin, C. and Chuntao, L. (2010). Application of Mu-Analysis for Evaluating the Robustness of RLV's Flight Control System, *IEEE International Conference on Electrical and Control Engineering (ICECE 2010)*, Wuhan, pp. 5027-5030.

Cook, M. V. (2007). *Flight dynamics principles*, Butterworth-Heinemann, Oxford, UK.

DoD (1990). *Flying Qualities of Piloted Aircraft*, Military Standard MIL-STD-1797A.

Gangsaas, D., Blight, J. and Caldeira, F. (2008). *Control Law Development for Aircraft: An Example from Industry Practice.* Tutorial Session, American Control Conference (ACC), Seattle, USA.

Gangsaas, D., Hodgkinson, J., Harden, C. Seeed, N. and Kaiming, C. (2008). *Multidisciplinary control law design and flight test demonstration on a business jet, Paper AIAA 2008-6489.* AIAA Guidance, Navigation and Control Conference and Exhibit, Honolulu, USA.

GARTEUR (1996). *Robust Flight Control Design Challenge Problem Formulation and Manual: The High Incidence Research Model (HIRM)*, GARTEUR/TP-088-4.

Hsu, K., Vincent, T., Wolodkin, G., Rangan, S. and Poolla, K. (2008). An LFT approach to parameter estimation, *Automatica* **44**(12): 3087-3092.

Menon, P.P., Postlethwaite, I., Bennani, S., Marcos, A. and Bates, D.G. (2009). Robustness analysis of a reusable launch vehicle flight control law, *Control Engineering Practice* **17**(7):751-765.

Menon, P.P., Bates, D.G., and Postlethwaite, I. (2007). Nonlinear robustness analysis of flight control laws for highly augmented aircraft, *Control Engineering Practice* **15**(6):655-662.

Natesan, K. and Bhat, M.S. (2007). Design and flight testing of Hinf lateral flight control for an unmanned air vehicle, *IEEE International Conference on Control Applications (CCA 2007)*, Singapore, pp. 892-897.

Ogata, K. (2002). *Modern Control Engineering*, Prentice Hall, Upper Saddle River, New Jersey, USA.

Pamadi, B. N. (2004). *Performance, stability, dynamics, and control of airplanes*, American Institute of Aeronautics and Astronautics, Inc., Reston, Virginia, USA.

Pfifer, H. and Hecker, S. (2011). Generation of Optimal Linear Parametric Models for LFT-Based Robust Stability Analysis and Control Design, *IEEE Transactions on Control Systems Technology* **19**(1): 118-131.

Phillips, W. F. (2004). *Mechanics of flight*, John Wiley and Sons, Hoboken, New Jersey, USA.

Roskam, J. (2003). *Airplane Flight Dynamics and Automatic Flight Controls I and II*, Design Analysis Research (DAR) Corporation, Lawrence, Kansas, USA.

Roskam, J. and Lan, C.-T. E. (2003). *Airplane aerodynamics and performance*, Design Analysis Research (DAR) Corporation, Lawrence, Kansas, USA.

Silva, A.S.F. (2009). *An approach to design feedback controllers for flight control systems employing the concepts of gain scheduling and optimization*, Master Thesis, Instituto Tecnológico de Aeronáutica (ITA), Brazil. Available from http://www.bd.bibl.ita.br/tesesdigitais/lista_resumo.php?num_tese=000552692 (last accessed on Feb 04th, 2011).

Skogestad, S. and Postlethwaite, I. (2007). *Multivariable Feedback Control – Analysis and Design*, John Wiley and Sons, Inc., New York, USA.

Stevens, B. L. and Lewis, F. L. (2003). *Aircraft Control and Simulation*, John Wiley and Sons, Inc, New York, USA.

Yechout, T.R. and Morris, S.L. (2003). *Introduction to aircraft flight mechanics: performance, static stability, dynamic stability, and classical feedback control*, American Institute of Aeronautics and Astronautics, Inc., Reston, Virginia, USA.

Yun, H. and Han, J. (2009). Robust flutter analysis of a nonlinear aeroelastic system with parametric uncertainties, *Aerospace Science and Technology* **13**: 139-149.

Zhou, X., Liu, L, Chen, Z. and Duan, H. (2007). Validation of Flight Control Law Based on LFT and Structured Singular Value, *Chinese Journal of Aeronautics* **20**(1): 60-65.